JOURNAL OF OPTOELECTRONICS AND ADVANCED MATERIALS, Vol. 12, No. 6, June 2010, p. 1372 - 1377

Microstructure and corrosion resistance for the electrodeposited nickel from watts-type baths

D. E. RUSU, A. ISPAS[a], A. BUND[a], C. GHEORGHIES[*], G. CÂRÂC
˝Dunarea de Jos˝ University Galati, Departments of Physics and Chemistry, Domneasca Str. 47, 800008 Galati, Romania
[a]Dresden University of Technology, Department of Physical Chemistry and Electrochemistry, Erich-Muller-Bau 66, D-01062 Dresden, Germany

Electrodeposition processes using direct current (DC) require the use of additives to control deposit structure and properties as well as current distribution. This work presents a study on the influence of electrodeposited nickel prepared from a Watts bath at different current density ranging from 1 Adm^{-2} to 10 Adm^{-2} at pH = 4. The structure of the nickel layers was investigated by scanning electron microscopy (SEM). Vickers hardness of deposited layers was also investigated. The electrochemical behaviour of the nickel layers was investigated by polarization potentiodynamic and electrochemical impedance spectroscopy methods. Protection level against corrosion was evaluated by polarization curves and Electrochemical Impedance Spectroscopy (EIS). Important results include the formation of uniform deposits showing fine grain and excellent protection against corrosion.

(Received April 28, 2010; accepted June 16, 2010)

Keywords: Nickel electrodeposition, Current density, Hardness, Corrosion resistance

1. Introduction

Nickel electrodeposited from a sulphate electrolytes has been used widely in many industrial fields to improve surface finishing, corrosion resistance and wear properties for various applications such as transport, and service apparatus, and to give the decorative and functionally suitable metal coatings[1-2].

Among all the studies, only a few have addressed the corrosion properties of electrodeposited nickel prepared from a Watts bath [3–6].Electrodeposited nickel shows an improvement in corrosion resistance with decreasing of grain size [3–5], but the opposite results are also obtained in the literature [6].Corrosion resistance can be affected by microstructure, such as grain size, surface morphology and texture, which is closely related to the electrodeposition parameters, such as current density, pH and electrolyte temperature.

A Watts bath is a most popular nickel electroplating bath and acid boric is an essential ingredient for controlling a bath pH and forming smooth and ductile deposits [7].

As it is known, the corrosion of acid solution on the metallic materials causes considerable losses. In order to reduce the corrosion of metal, several techniques have been applied [8]. For example, anodic or cathodic protection, coating layer on the metal, oxidizing or phosphatizing treatment, the application of inhibitors and inhibiting materials etc.

Therefore, in the present work the aim was to prepare the electrodeposited nickel using a Watts bath operating under different conditions, such us bath composition, plating current densities, temperature and plating time to find the optimum conditions for producing sound and satisfactory deposits. On the basis of the analysis of the microstructure of electrodeposited nickel, the corrosion behaviour was analyzed by electrochemical impedance spectroscopy and polarization methods in 0.5M Na_2SO_4 solution pH = 2.

2. Experimental procedure

The plating was carried out in Watts baths with and without additives. Composition and operation conditions for each bath are listed in Tables 1.The suspension bath was stirred by mechanical stirrer (250-300 rpm). The temperature was controlled with a Haake thermostat (model GD1, accuracy ±1 °C). The cathode, a cooper disc with an area of 2.26 cm^2, was vertically centred and surrounded by a cylindrical nickel counter electrode.

The cooper substrates was mechanically polished with different grades of emery papers (800,1200,2400 and 4000), electrochemically degreased in an alkaline bath UNAR EL 63 solution (commercial product from Schering Germany) at 3V and 0,2 A dm^{-2} for 20-30 seconds and activated at room temperature with HCl 1N solution then rinsed with doubly-distilled water, dried with pressured air.

A saturated calomel electrode (SCE) was used as the reference electrode. The electrodeposition was carried out using a potentiostat/galvanostat (EG & G model 263A, SUA) with a current density between 1 and 10 A dm^{-2}. The electrodeposits with the thickness of about 250 μm were obtained for two hour time deposition. After

electrodeposition process the samples were rinsed with doubly-distilled water, dried with pressured air.

The cathode current efficiency CCE) was calculated based on the difference of mass of specimen before and after the plating ($\eta=m_{exp}/m_{theo}$). Where m_{exp} is the mass of the deposit obtained experimentally and m_{theo} is the theoretically mass of the deposit determined by calculation of the quality of the electricity passing through the cell with a copper coulometer according to Faraday's law.

For a better adhesion of the nickel layers at substrate, copper substrates were initially immersed for ten minutes in a solution of $NiSO_4 \cdot 6H_2O$ having a concentration of 263 gl^{-1}, pH = 2 and potentiostatically polarized at U=1V. For pH adjust, H_2SO4 conc.98 % and $NaHCO_3$ purity 99.5% were used.

Table 1. Compositions and working parameters for nickel Watts baths.

Parameters	Values
$NiSO_4 \cdot 6H_2O$	0.9 M
$NiCl_2 \cdot 6H_2O$	0.21 M
H_3BO_3	0.48 M
Sodium dodecyl sulfate ($C_{12}H_{25}SO_4Na$) -SDS-	0.1 gl^{-1}
Temperature	50 ºC
Current density	1, 2, 5, 10 Adm^{-2}
Time	15, 30, 60, 120 min
pH	4.0 ±0,2

The surface morphologies of the electrodeposits were characterized by scanning electron microscopy (SEM Zeiss SEM DSM 982 (Oberkochen, Germany).

X-ray diffraction analyses were performed at room temperature on Siemens D 5000 equipment allowing estimation the grain size and the texture degree of the deposits. The scan rate was $0.12°min^{-1}$ over a two-theta range from 10 to 100°.The Debye–Scherrer relation in the (200) reflection was used for estimating the crystallite size of nickel films [9]. The texture of the nickel films in the $[hk\ell]_i$ crystallographic direction was estimated using the relative texture coefficient $RTC_{(hk\ell)_i}$.

$$RTC_{(hk\ell)_i} = \frac{\left(I_{hk\ell} / I^0_{hk\ell}\right)_i}{\frac{1}{5}\sum_{i=1}^{5}\left(I_{hk\ell} / I^0_{hk\ell}\right)_i} \times 100\%$$

where $I_{hk\ell} / I^o_{hk\ell}$ is the relative intensity of the $(hk\ell)$ reflection, and $\sum_{i=1}^{5}\left(I_{hk\ell} / I^0_{hk\ell}\right)_i$ is the sum of all relative intensities for (111),(200),(220),(311) and (222) lines. The superscript 0 refers to the intensities of a randomly oriented nickel powder sample (JCPDSno.4-850).

The hardness of the samples was determined with a Vickers microhardness device (Fischer Scope HM 2000 S) as described in DIN EN ISO14577. The recorded values are averages of 10 measurements performed on different locations in the centre section of each sample. The thickness of all coatings is more than ten times the maximum indentation depth of 1 μm in order to reduce effects of the substrates.

For electrochemical corrosion measurements, a Potentiostat / Galvanostat / ZRA Gamry reference 600, with three electrodes, namely: working electrode (WE) is substrate of nickel, a platinum electrode as auxiliary electrode (EC) and a saturated calomel electrode as reference electrode (RE) (E_0 = 0.241 V vs. SHE or E_{ref} = 241.2 mV vs. NHE) were used. As a test solution was used a solution of 0.5 M Na_2SO_4 at temperature room (25± 1°C).

EIS measurements used in the initial frequency (IF) of 10^5Hz, the final frequency (FF) of 0.1 Hz, 10 mV AC amplitude wave, and 1s delay before integration. Impedance spectra were recorded on different samples after different immersion times (10 min, 30 min, 1h, 2h, 4h, 6h, 24h and 30h). All recorded spectra were analyzed in the impedance Nyquist diagrams. PD measurements (polarization curves) were used for initial and final potential, according to OCP and scan rate of 1mV/s. Potentiodynamic polarization curves were recorded after 30 min and 1 h of immersion. The corrosion current density (*i*corr) for the particular specimens was determined by extrapolating the anode and cathode Tafel curves.

3. Results and discussion

3.1. Current efficiency

The current efficiency for nickel electro-deposition from the Watth bath is given in fig.1 to different temperature and deposition time effect. The data indicate that the CCE depends strongly on Ni content in the bath. For nickel samples deposited at a temperature of 50ºC, current efficiency higher than 95% have been achieved starting from a current density of 5 A/dm^2, the CCE increases markedly with the increase of nickel time and current in the bath. For depositions made at 900 s, the current efficiency is lower for small current density of about 1 A/dm^2, it being 86.5%.

With increasing deposition time current efficiencies bigger than 96% were obtain. Lowest current efficiencies are obtained when the time of deposition was 900s, but the current efficiency increases in case of using SDS, with almost 10%, which explains the additive role in reducing surface tensions in the electrolyte and the stress during crystallization of nickel deposits.

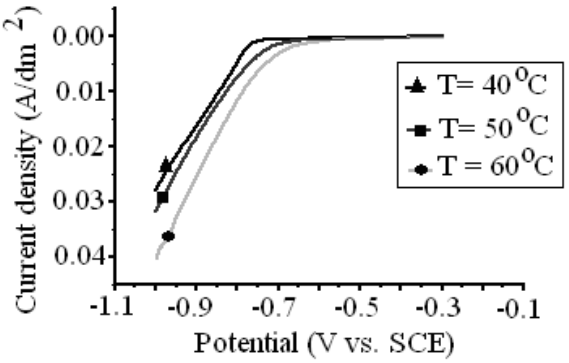

Fig. 1. Cyclic voltammograms of Ni layers for different temperature in sulphat bath. Scan rate was 5 mV/s.

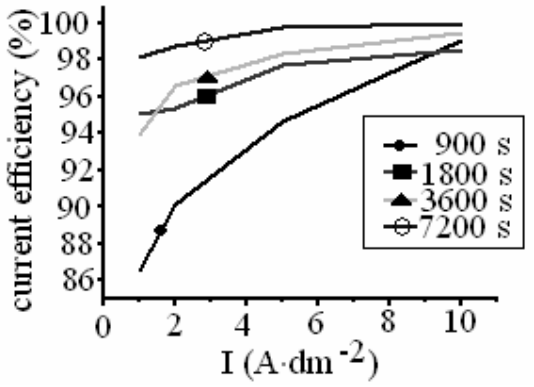

Fig 2. Current efficiency as a function of the applied current density corresponding to a different deposit time.

3.2. Deposit morphology and crystallographic orientation

The microstructures of electrodepositednickel coating were determined by scanning electron microscope (SEM). SEM images taken for all samples of nickel deposits indicate significant structural changes made at different times and current densities. The typical SEM for the nickel electrodeposits are show in Fig. 3.

For current density of 10 Adm^{-2} which was the highest value tested, at a temperature of 50°C is observed thread-like appearance of the structure. At a same temperature of 50°C, pure nickel crystals grow in size with increasing current density because of the higher deposition rate for crystallization. Morphology of the deposition changed with the increasing current density. Where as at 1 Adm^{-2} one can distinct separation of large crystals formed. Crystals formed at 5 Adm^{-2} tend to shrink, while from 10 Adm^{-2} small crystals morphologically well defined, are observed this future is not preserved for 1 Adm^{-2} and 2 Adm^{-2}.

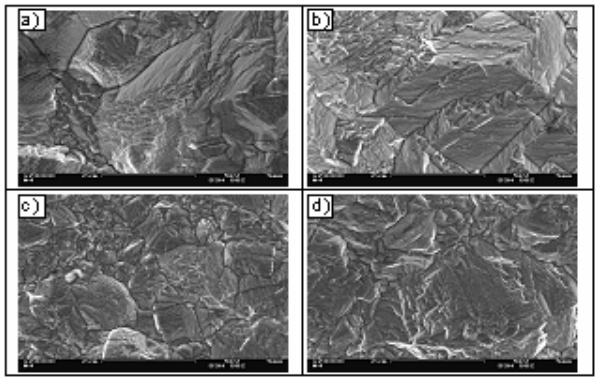

Fig.3 Surface morphologies of electrodeposited nickel at different current densities: a) 1A/dm^2; b) 2 A/dm^2; c) 5 A/dm^2; d) 10 A/dm^2.

The XRD patterns of electrodeposited nickel are show in Fig. 4. All the electrodeposits consist of grains with a strong (200) plane and a weak (111) plane. Preferred orientation is represented by the X-ray peak ratio of I(200)/I(111). Grain size is assessed by the Debye-Scherrer equation. The values of the preferred orientation and grain size are tabulated in Table 2. In addition, a relatively strong (200) texture for 10 A dm^{-2} is associated with large grain size. Increasing current density leads to an increase in grain size, which results from the evolution of more hydrogen at the cathode interface [10]. The modification of the growth interface by hydrogen changes the surface energy and growth mechanisms, and then facilitates the formation of larger grain size.

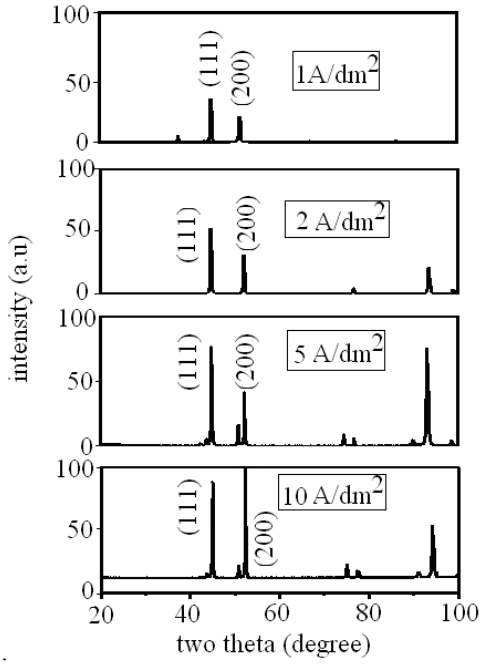

Fig.4. XRD patterns of electrodeposition prepared at different current density.

Table 2. Preferred orientation and grain size in [110] and [200] crystallographic directions for electrodeposited nickel in sulphate bath

Current density	$I_{(200)}/I_{(111)}$	Grain size (nm)	
		[111]	[200]
1 A dm^{-2}	0.595584	128	78
2 A dm^{-2}	0.268003	97	56
5 A dm^{-2}	0.486428	122	78
10 A dm^{-2}	1.92553	187	194

3.3. Microhardness measurements

Ten measurements were conducted on each sample and the results were averaged. Microhardness of pure nickel samples deposited at different current densities and at different times of deposition was tested. Errors of the measurements were comparable. Average hardness values between 250-450 HV. The same trend of increasing or decreasing of the hardness was noticed with increasing deposition time, and the errors of the measurements were ± 50 HV. With increasing temperatures lower values of HV obtained independently of the deposition time. Microhardness of nickel layers vs. current density (a) and plating time (b) in figures 5a and 5b are displayed.

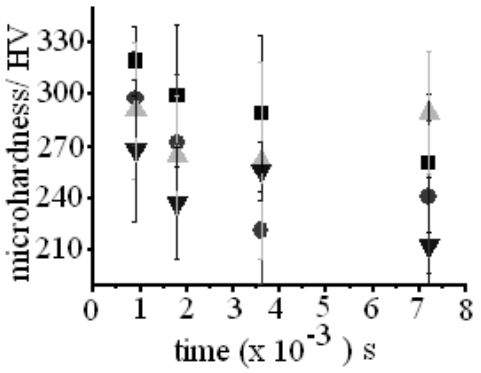

Fig. 5a) Microhardness as a function of the electrodeposition time for different current densities (■) 1 A dm^{-2} , (●)2 A dm^{-2}, (▲)5 A dm^{-2} , (▼)10 A dm^{-2}

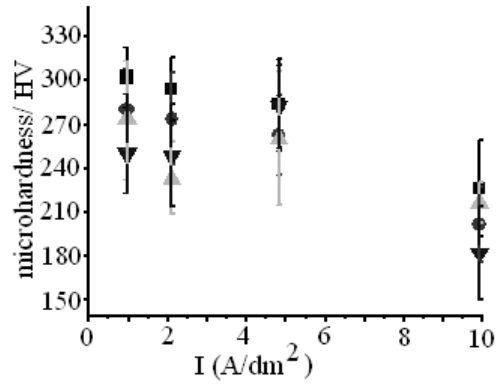

Fig.5b) Microhardness as a function of the current density for different deposition time (■) 900 s , (●)1800 s, (▲)3600s , (▼)7200s

3. 4. Potentiodynamic polarization studies

Figs. 6 indicate the polarization curves of cooper substrate with Ni alloy coatings to different current densities to corrosive medium consisting to 0.5M Na_2SO_4 solution having pH2. All the curves display the active-passive-transpassive behaviour between -0.5 V and 0V with different values of the electrochemical parameters. It indicates that the mechanism of activity and passivation is similar in essence for all electrodeposited tested for 30 min. and 1 h. The current density increases with increasing potential in the active area. Then the electrode passivates and displays high stability, as characterized by low and steady value of passive current density. Furthermore, the oxide film breaks down as demonstrated by an obvious increase in current density in the transpassive region correspondingly, the pitting corrosion occurs.

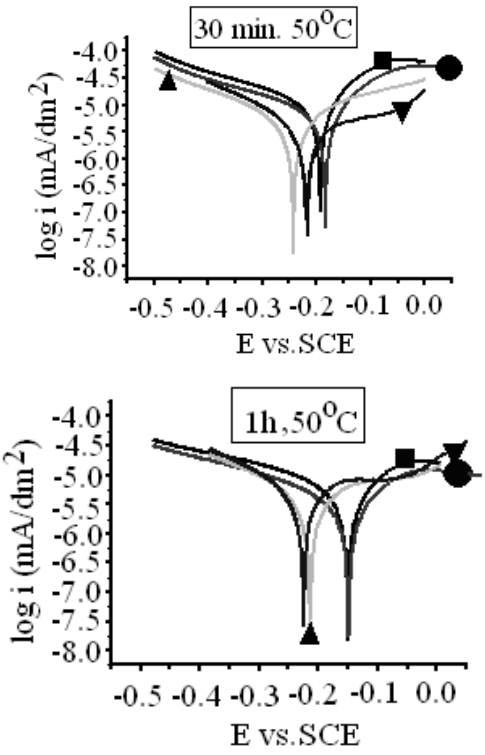

Fig. 6 . Comparative potentiodynamic diagrams of nickel deposited for 1 h after 30 min and 1h from immersion time, at different current density (■) 1 A dm^{-2} , (●)2 A dm^{-2}, (▲)5 A dm^{-2} , (▼)10 A dm^{-2}

The corrosion current density (i_{corr}) and corrosion potential (E_{corr}) are calculated from the intercept of the Tafel slops. Polarization resistance (R_p) and the corrosion rate (in mm/year) are estimated from the polarization curves, and then tabulated in Table 4. Among all the samples to 2 and 5 A dm^{-2} exhibits the lowest values of i_{corr} and R_p. As for 1 and 10 A dm^{-2} both i_{corr} and R_p increase with increasing time and current density used to prepare electrodeposition. However, the variation of E_{corr} is opposite to the variation of i_{corr} and Rp. Therefore, the electrodeposition to 5 A dm^{-2} exhibits the best corrosion resistance, which is attributed to the compact structure.

3.4. Electrochemical impedance spectroscopy

The Nyquist plot representations of impedance spectra performed in 0.5M Na_2SO_4 solution pH = 2, at different times of immersion and current density are shown in Fig. 7.

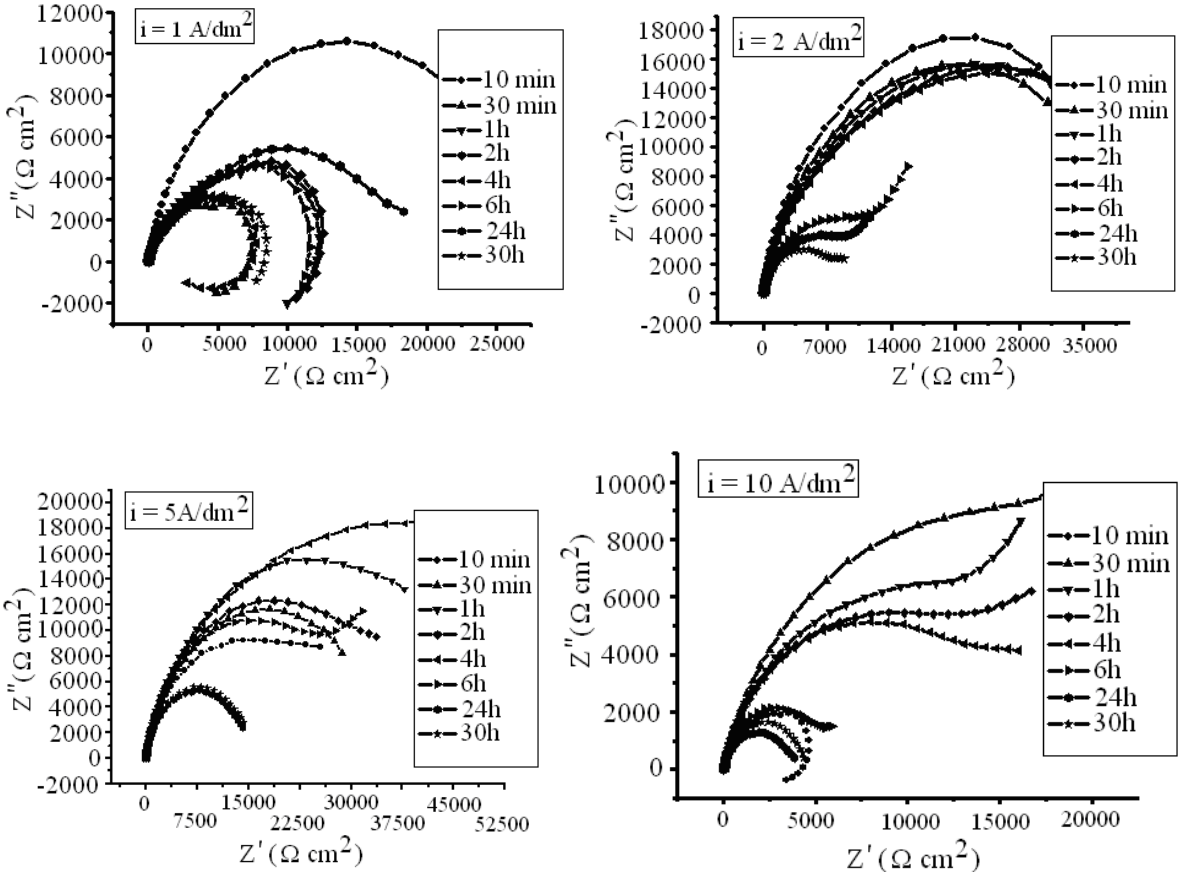

Fig.7. Nyquist diagrams of impedance spectrum for Nickel deposits in 0.5M Na_2SO_4 at different current densities.

An equivalent electrical circuit was proposed to account for the experimental impedance spectra [10]. The impedance plots exhibit depressed semicircles, corresponding to a charge-transfer resistance in parallel with an equivalent capacitance. The equivalent circuit, as shown in Fig 8, is used to fit the corrosion resistance parameters. In addition, a constant phase element (CPE) is used as a substitute for the capacitor to fit the impedance data of the electrochemical double-layer capacitance, which is ascribed to the imperfect surface of the electrode [11].

The fitted impedance spectra are in good agreement with the impedance spectra recorded during the measurements as shown in Fig 7 the calculated values of circuit elements are listed in Table 3. It can be found that all fitted corrosion parameters of the electrodeposits vary with the change microstructure. The polarization resistance for 2 A dm^{-2} is greater than that of other samples. The corrosion resistance decreases, but the constant phase element (CPE) increases with current density used to prepare the electrodeposits except samples deposits to 2 A dm^{-2}, which agrees with the results of potentiodynamic polarization tests.

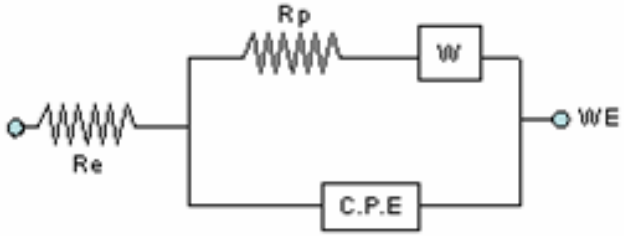

Fig. 8. An equivalent circuit for impedance measurement for nickel deposits from Watts bath.

Table 3. Polarization resistance and capacitance values of nickel layers in sulphate bath for different time of immersion calculated with equivalent circuit from Fig.8.

Current density	Data obtained from impedance spectra	Immersion time							
		10 min	30 min	1 h	2 h	4 h	6 h	24 h	30 h
1 Adm^{-2}	Rp ($k\Omega\ cm^2$)	27.26	8.56	13.48	13.75	8.63	14.67	18.03	8.44
	CPE ($\mu F/cm^2$)	10.76	20.80	26.45	18.96	14.32	29.76	20.81	14.76
2 Adm^{-2}	Rp ($k\Omega\ cm^2$)	40.77	40.88	45.88	43.87	43.56	15.49	12.12	8.972
	CPE ($\mu F/cm^2$)	8.936	12.00	15.26	16.42	16.01	10.80	18.52	22.63
5 Adm^{-2}	Rp ($k\Omega\ cm^2$)	30.31	33.66	43.74	33.29	52.03	32.23	14.40	14.95
	CPE ($\mu F/cm^2$)	17.63	13.22	9.63	15.78	6.74	5.64	13.37	15.75
10 Adm^{-2}	Rp ($k\Omega\ cm^2$)	4.55	23.96	19.84	16.48	15.82	5.79	3.56	4.35
	CPE ($\mu F/cm^2$)	24.02	17.91	18.50	11.67	10.48	16.92	52.33	51.37

4. Conclusions

Nickel layers were electrodeposited from Watts bath for different deposition conditions: current densities and deposition times.

Higher current efficiencies were obtained for higher current densities and longer deposition times;

Microstructure of deposits has changed with changing current density and operating times;

Microhardness of the layers is lower at higher temperatures;

Electrodeposited nickel prepared at 2 and 5 A dm-2 is provided with the best corrosion resistance. The corrosion depends on the electrodeposition parameters;

Varying the deposition parameters induced changes in structure and properties of the deposit.

Acknowledgements

This work was supported by Project SOP HRD - SIMBAD 6853, 1.5/S/15 - 01.10.2008 and financial support within the project PNII-PCE- ID no 2290.

References

[1] A. M. El-Sherik, U. Erb, J. Mater. Sci. **30,** 5743, (1995).
[2] J. R. Tuck, A. M. Korsunsky, R. I. Davidson, S. J. Bull, D. M. Elliott, Surf. Coat. Technol. **127,** 1 (2000).
[3] K. C. Chan, W. K. Chan, N. S. Qu, J. Mater. Process. Technol. **447**, 89 (1999).
[4] R. Mishra, R. Balasubramaniam, Corros. Sci. **46,** 3019 (2004).
[5] S. H. Kim, U. Erb, K. T. Aust, F. Gonzalez, G. Palumbo, Plat. Surf. Finish. **91,** 68 (2004).
[6] J. H. Qiu, Mat. Sci. Forum**, 211**, (2003).
[7] R. Rofagha, R. Langer, A. M. El-Sherik, U. Erb, G. Palumbo, K. T. Aust, Scr. Metall. **25,** 2867 (1991).
[8] S. W. Banovic, K. Barmak, A.R. Marder, J. Mater. Sci. **33**, 639 (1998).
[9] C. Gheorghies, Analiza Structurii Fine a Materialelor, Ed. CERMI, Iasi, 2007.
[10] L. Lemoine, F. Wenger, J. Galland, Special Technical Publication, ASTM **1065**, Philadelphia, USA, (1990).
[11] A. V. Benedetti, P. T. A. Sumodjo, K. Nobe, P. L. Cabot, W.G. Proud, Electrochim. Acta **40,** 2657 (1995).
[12] C. Gheorghies, I. V. Stasi, C. C. Lalau, J. Optoelectron. Adv. Mater. **11**(2) 146 (2009).

*Corresponding author: cgheorg@ugal.ro